International Information and
Engineering Technology Association
Advancing the World of Information and Engineering

Identification of Apnea-Hypopnea Index Subgroups Based on Multifractal Detrended Fluctuation Analysis and Nasal Cannula Airflow Signals

Fatma Z. Göğüş[1*], Gülay Tezel[1], Seral Özşen[2], Serkan Küççüktürk[3], Hülya Vatansev[4], Yasin Koca[2]

[1] Department of Computer Engineering, Konya Technical University, Konya 42075, Turkey
[2] Department of Electrical Electronics Engineering, Konya Technical University, Konya 42075, Turkey
[3] Department of Medical Biology, Necmettin Erbakan University, Konya 42090, Turkey
[4] Department of Chest Diseases, Meram Medical Faculty, Necmettin Erbakan University, Konya 42090, Turkey

Corresponding Author Email: fzgogus@ktun.edu.tr

ABSTRACT

The diagnosis of obstructive sleep apnea hypopnea syndrome (OSASH) and making decision of treatment necessity with positive airway pressure (PAP) therapy are time consuming and costly processes. There were different approaches in literature to accomplish these processes successfully and as soon as possible by using physiological signals with selected feature extraction and machine learning techniques. To reach fastest and true result, selection of optimal physiological signal(s), feature extraction and learning techniques is important. This study aimed to identify apnea hypopnea index (AHI) subgroups of 120 subjects and thus diagnose of OSASH and determine the need for PAP therapy by applying Multifractal Detrended Fluctuation Analysis (MDFA) as a feature extraction technique to only single channel nasal cannula airflow signals. After the extracted features from airflow signals with MDFA were gone through feature selection phase, the selected features were evaluated in Random Forest classifier. With the implementation of all processes, OSAHS patients were discriminated from healthy subjects with 95.83% accuracy, 96.88% sensitivity and 93.75% specificity. 93.75% sensitivities and 93.75%, 100% and 96.88% specificities were obtained for 15≤AHI (PAP therapy necessary), 5≤AHI<15 (require additional information for PAP therapy decision) and AHI <5 (not require PAP therapy) subgroups, respectively.

1. INTRODUCTION

Positive Airway Pressure (PAP) therapy is the most effective and widely accepted treatment for Obstructive Sleep Apnea Hypopnea Syndrome (OSAHS) [1, 2]. PAP therapy aims to keep open the upper airways of patients during night, regulate breathing and sleep quality, decrease daytime sleepiness, improve attention and decrease risk of major other diseases [3]. Positive pressure applied to the upper airways eliminates negative pressure, and thus prevents apnea, hypopnea, snoring and current restriction [4]. However, in order to provide the effective PAP therapy, early diagnosis of OSAHS should be carried out and then OSAHS patients that require the therapy should be determined [5]. According to the guideline published for PAP therapy by the Centers for Medicare and Medicaid Services (CMS) in the United States [6], PAP therapy is the standard treatment for OSAHS when the Apnea-Hypopnea Index (AHI) is greater than or equal to 15 events per hour [6]. This therapy is recommended to patients with 5≤AHI<15 if patients are accompanied by excessive daytime sleepiness, impaired neurocognitive function, mood disorders, insomnia, cardiovascular disease (e.g., hypertension, ischemic heart disease), or a history of stroke [6]. If the clinical complaints of the patients are not obvious, their AHI values are between 5 and 15, and there are no additional risk factors, general recommendations are preferred for the treatment of patients without the need for PAP therapy. If the AHI values of individuals are less than 5, it means that individuals are not diagnosed with OSAHS and PAP therapy is not required.

In the clinical environment, AHI values of patients are identified through overnight polysomnography (PSG). It requires patients to spend one night in the laboratory and recording of their multiple physiological signals including brain waves (electroencephalogram-EEG), eye movements (electrooculogram-EOG), chin muscle activity (chin electromyogram-EMG), airflow from the nose and mouth, chest and abdominal movement, blood oxygen levels (oximetry-SpO2), heart rate and rhythm (electrocardiogram-ECG), and leg movements (leg electromyogram-EMG) simultaneously [7]. These recorded signals are interpreted by sleep specialists according to the American Academy of Sleep Medicine (AASM) guideline [8] and AHI values are calculated based on the number of patients' apnea and hypopnea events per hour of sleep. According to the calculated AHI values, patients who will also spend the next night in the sleep laboratory for the implementation of PAP therapy are determined.

The processes of obtaining physiological signals, detecting each apnea and hypopnea event, calculating AHI, diagnosing and determining the patients that require PAP therapy according to this calculation are time consuming, laborious, boring, exhausting, person-dependent and costly [9, 10]. In addition, PSG and sleep laboratories show limited availability

in some places around the world. This situation results in long waiting lists, thus delaying the diagnosis and treatment of the patients affected by this syndrome [7]. For these reasons, several researches and studies producing alternative techniques has been performed to simplify and to automate these processes and to decrease time spent on these processes in recent years. A group of these studies [5, 10-24] used airflow signals by considering the first condition of AASM [8], which is the necessity of certain reduction in airflow to identify apnea and hypopnea events [8]. These studies carried out both OSAHS diagnosis and determination of need for PAP therapy of individuals either by detecting the apnea-hypopnea events with the algorithm developed by using airflow signals in small segments [10-12, 14, 15, 18-25], or by using various feature extraction techniques (nonlinear, time, frequency etc.) and classification algorithms such as C4.5 Decision Tree, Artificial Neural Network (ANN), Support Vector Machine (SVM), Random Forest (RF) [5, 13, 17]. All these studies have been promising and encouraging that the procedures performed in the clinic environment can be automated successfully, and also proved that airflow signals are the primary indicators of OSAHS. Therefore, this study aimed to determine automatically whether the people who admitted to the clinic with suspicious of sleep syndrome had OSAHS or not and whether they needed treatment with PAP therapy or not by identifying their AHI subgroups. To achieve these objectives, it was proposed to evaluate single-channel nasal cannula airflow signals with novel features extracted with an effective technique and a classification algorithm.

Since the sleep disordered breathing occurs as a result of a combination of anatomical upper airway predisposition and changes in neural activation mechanisms [14], overnight airflow signal records exhibit nonlinear dynamics and have variations. These signals can also show scale invariant structure in other words the structure can repeat itself on subintervals of signal. For this reason, structural characteristics of physiological airflow signals are not always represented with classical measures such as average amplitude, Fourier Transform based features, statistical features, etc. used in previous studies [13, 17]. In such cases, utilizing nonlinear and fractal approaches such as Multifractal Detrended Fluctuation Analysis (MDFA) is useful for discovering the characteristics of these signals. In literature, MDFA technique was applied to various physiological signals to differentiate pathological conditions from normal. Some of these studies carried out with miscellaneous signals by employing MDFA can be given as detection of epileptic seizure by using EEG [26], heart disease by using heart sounds [27], human gait diseases by using human gait time series [28]. To date, no study has not existed using the MDFA technique to explore OSAHS, but some researchers have preferred Detrended Fluctuation Analysis (DFA) which has been widely used for the representation of monofractal scaling features in physiological signals to assist OSAS diagnoses [5, 7, 29, 30]. Vaquerizo-Villar et al. stated that apnea and hypopnea events produced random spikes and/or irregular fluctuations in the SpO2 signals. So, they used DFA with SpO2 signals for pediatric OSAHS diagnosis [7]. Da Silva et al. [29] and Deng et al. [30] preferred DFA that was able to detect long-range correlations in noisy, nonstationary time series for heart rate

analysis in OSASH. Kaimakamis et al. [5] used three signals including nasal cannula flow, thoracic belt and SpO2 signals for OSAHS. However, they utilized DFA for only two respiratory signals (nasal cannula flow and thoracic belt). Although the nasal cannula airflow signal was included in the analysis of OSAHS in their study, additional signals were also used as supportive.

As a result of literature investigation, it was seen that although DFA were utilized in studies by some researches, there were no studies focused on OSAHS diagnosis or determination the need for PAP therapy by applying MDFA technique to nasal cannula airflow recordings. However, the structure of many physiological signals, including nasal cannula airflow, shows spatial and temporal variations. In addition, as stated by Vaquerizo-Villar et al. [7], apnea and hypopnea events in OSAHS patients produce random spikes and/or irregular fluctuations in their physiological signals. These variations and fluctuations are compatible with multifractal structure and cannot be characterized completely by single fractal provided with conventional DFA. Therefore, MDFA, the generalized version of the DFA technique, is more suitable for the analysis of signals contain such variations and fluctuations. Considering this fact, in this study MDFA technique was preferred as a feature extraction method to reveal additional significant information from airflow signals. Thus, this study would provide novelty to the literature by analyzing multifractal characteristics of airflow signals in OSAHS patients, which have not been reported in existing literature.

Within the scope of the study, after analysis of nasal cannula airflow signal of each person was performed by using MDFA technique, MDFA based novel features were extracted. Then, each person was assigned to one of the AHI subgroups with either AHI<5 or 5≤AHI<15 or 15≤AHI by using extracted MDFA based features and Random Forest (RF) classifier. As a result of the study, people with AHI <5 were determined as non-OSAHS, that is, healthy individuals, and others were diagnosed as OSAHS automatically. In addition, it was decided that PAP therapy was absolutely required for patients with 15≤ AHI according to CMS guideline [6]. For patients with an AHI between 5 and 15, it was concluded that additional information was needed proposed by CMS [6] to decide treatment with PAP therapy. Therefore, it was suggested that PAP therapy decision of these patients should be left to sleep specialists to investigate additional information recommended by the CMS [6].

This study will support a low-cost PSG device that patients can use in their own home, as it automates the processes of diagnosing OSAHS and determining the need for PAP therapy. In this way, it will eliminate the need to stay in the laboratory for these processes and will save time and cost.

2. MATERIALS AND METHODS

This study focused on the identification of different AHI subgroups (AHI <5, 5≤ AHI <15, 15≤ AHI) and thus the diagnosis of OSAHS and determination the necessity of treatment with PAP therapy. Figure 1 demonstrated the flow diagram of procedures performed throughout this study.
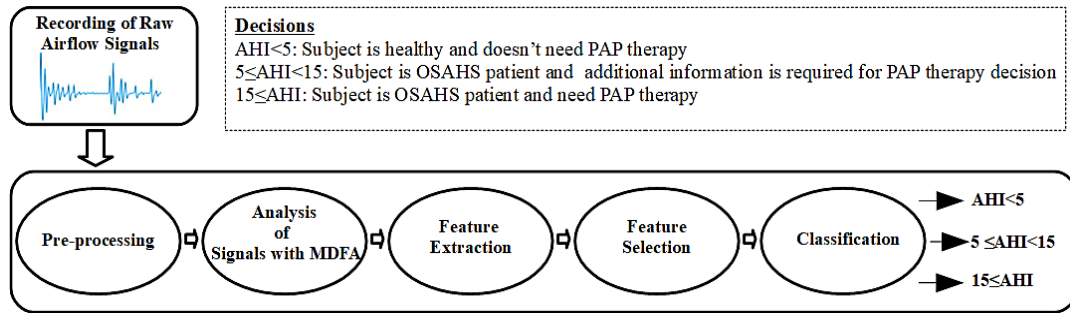
Figure 1. Flow diagram of study

The study consists of 6 main steps shown in Figure 1. Primarily, raw nasal cannula airflow signals of subjects to be evaluated under this study were recorded by a PSG device in clinic. Then, pre-processing operations, filtering and adaptive normalization, were carried out on recorded signals to obtain accurate results. Once the signals were ready by pre-processing, MDFA technique was applied to the airflow signals of subjects and multifractal spectra were created. In the feature extraction step, 23 novel features were extracted from every multifractal spectrum created for each subject. Subsequently, 5 feature selection methods, i.e., Information Gain Attribute Evaluation, Correlation Attribute Evaluation, OneR Attribute Evaluation, Cfs Subset Evaluation and Wrapper Subset Evaluation were applied to the extracted features separately. In this way, the most effective features on the identification of different AHI subgroups were found by each selection method according to its own criteria. Finally, the classification procedure was realized to classify subjects into different AHI subgroups using selected features and RF algorithm. According to AHI subgroup identified as a result of the classification, it was decided that subjects were OSAHS or healthy and they were required treatment with PAP therapy or not.

2.1 Data acquisition

120 subjects admitted to the Necmettin Erbakan University, Meram Faculty of Medicine, Department of Chest Diseases, Sleep Laboratory with complaints of sleep disorders were included in this study. The experimental protocol conformed to the principles outlined in the Declaration of Helsinki, with an approval statement confirmed by the Medical Ethics Review Board (Faculty of Medicine, Selcuk University, Konya, Turkey) for institutional, non-invasive clinical research. All participants provided proper informed consent. All subjects underwent standard PSG with Philips Respironics Alice 6 (sleepware G3 version 3.9.3 software) that recorded physiological signals including nasal cannula airflow signal with 100 Hz sampling frequency.

33 subjects are healthy, so their AHI values less than 5. 87 subjects are suffered from the OSASH. 33 of these OSAHS subjects are in the group of $5 \leq AHI < 15$. Another 25 OSAHS subjects are in the group of $15 \leq AHI < 30$ and the AHI values of the remaining 29 subjects are equal to or greater than 30.

In total, 54 subjects have AHI values greater than or equal to 15 and need PAP therapy as the standard treatment of OSAHS. For PAP therapy decision of 33 subjects whose AHI values are between 5 and 15, other information such as excessive daytime sleepiness, insomnia, cardiovascular disease etc. are need to be examined. 33 subjects with an AHI less than 5 are healthy and do not require PAP therapy.

2.2 Pre-processing

A third-order Butterworth bandpass filter with cut-off frequencies of 0.01–0.7 Hz was applied to airflow signals by trying different filters with various frequency ranges mentioned in previous studies [18, 19, 23, 31].

Airflow signals are long-term records and can be affected by sensor, body posture, or patient movements during measurements and thus they may change over time. Therefore, the airflow signals of the subjects in this study were normalized by using an adaptive normalization method [12, 24].

Following the pre-processing, subjects in each AHI subgroup were randomly divided into two groups, training and test. Approximately 60% of the subjects constituted the training group and 40% of them were reserved as the test group.

2.3 Analysis of airflow signals by MDFA

In 1995, Peng et al. [32] proposed DFA for detecting the long range correlation of DNA sequences. Since that time, this technique has frequently used to determine mono-fractal scaling features in non-stationary signals [5, 7, 29, 30]. However, many physiological signals can show scale invariant structure and may not exhibit mono-fractal characteristic [33]. Therefore, these signals cannot be analyzed with a single scaling exponent and can require different many scaling exponents [34]. Due to this requirement, MDFA was developed by Kantelhardt et al. [33] in 2002. Thus, shortcomings of DFA were eliminated by MDFA for multi-fractal signals.

The detailed description and algorithm of this technique can be found in the literature [26, 28, 35, 36]. The main steps of MDFA are [37]:

✓ Computing the mean of the time series

✓ Computing the integrated time series by summing the differences obtained by subtracting the mean value from each value in the series

✓ Fragmentation of integrated time series and computing the local Root-Mean-Square (RMS) variation/trend

✓ Finding local detrending of the time series

✓ Computing multifractal detrending, q-order RMS (qRMS)

✓ Computing q-order Hurst exponent (Hq) and q order mass exponent (tq)

✓ Computing q-order singularity exponent (hq) and q-order singularity dimension (Dq)

✓ Creating the Multifractal Spectrum (the plot of hq versus Dq)

In this study, adaptive normalized nasal cannula airflow signals were analyzed with MDFA technique and thus

multifractal spectra were created. Since the appropriate choice of q in most biomedical physiological signals was between -5 and 5 [35, 38], q was chosen to vary between -5 and 5 in steps of 0.1 for the MDFA technique used in this study. The value of s (scale) was determined to be between 16 and 1024. These scale range have a total number of 19 equal intervals in between 16 and 1024, spaced logarithmically. According to these parameters multifractal analysis of each subject's airflow signal was carried out. Figure 2 shows the q-order Hurst exponent. As seen from the Figure 2, curve-shaped Hurst exponent plots are in a nonlinear relationship with q values for all AHI subgroups. This figure shows that airflow signals of subjects in different AHI subgroups exhibit multifractal nature.

In the MDFA technique, Hq is converted into q-order Mass exponent (tq) firstly [37]. Figure 3 indicates q-order Mass exponents for all AHI subgroups in this study. It can be seen from Figure 3 that Mass exponent dependent on q shows a curve shape, especially for the group $15 \leq$ AHI. This means that as the value of AHI increases, the airflow signals display a more nonlinear multifractal structure and large fluctuations.
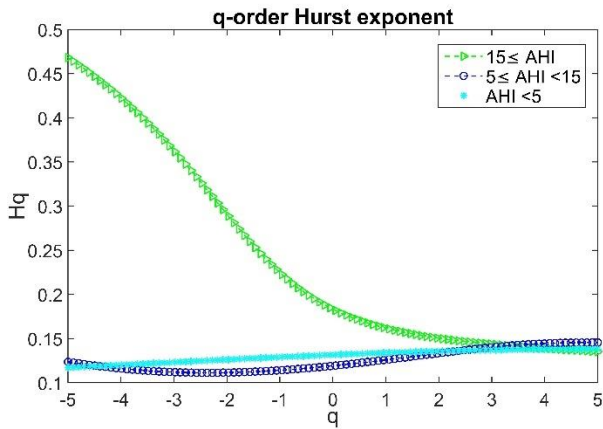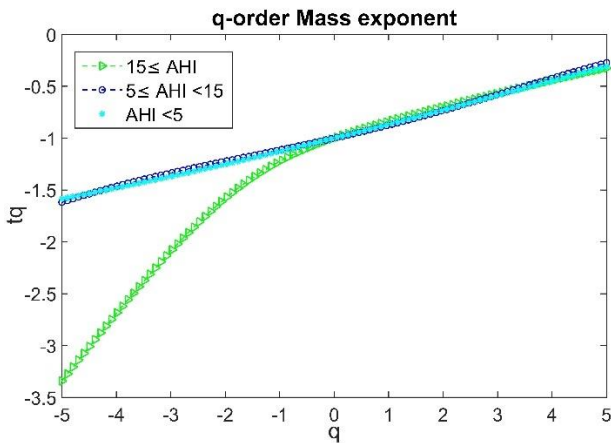

Figure 2. q-order Hurst exponent

Figure 3. q-order Mass exponent

The tq is used to compute the q-order singularity exponent (hq) and the q-order singularity dimension (Dq) [35]. The plot of hq versus Dq is the Multifractal Spectrum [37]. Multifractal Spectrums of patients in different AHI groups are as in the Figure 4. As seen in Figure 4, patients in different AHI subgroups have different types of spectra. While right-skewed spectrum which is related to relatively strongly weighted high fractal exponents is observed for patient with $15 \leq$ AHI (Figure 4. a.), left-skewed spectrum which is indicative of low fractal

exponents is seen for healthy person with AHI<5 (Figure 4. c.). For a patient with an AHI between 5 and 15, a spectrum skewed on both sides is observed (Figure 4. b.). Therefore, it can be said that multifractal spectra of airflow signals and spectra' different features may be useful for distinguishing OSAHS patients belonging to different AHI subgroups.

2.4 Feature extraction based on MDFA

After the multifractal spectra were created for airflow signals of subjects through the MDFA technique, following novel 23 features were extracted from the spectra.

F1: The mean of Hurst exponents calculated for each q value ranging from -5 to 5 as in Eq. (1). N is the number of q: -5 to 5 in steps of 0.1.

$$\frac{1}{N} \sum_{q=-5}^{5} Hq \qquad (1)$$

F2: Maximum Hurst exponent value (Hq_{max}).
F3: Minimum Hurst exponent value (Hq_{min}).
F4: Generalized Hurst exponent.
F5: Multifractal spectrum width calculated with Eq. (2).

$$MS_{width} = hq_{max} - hq_{min} \qquad (2)$$

F6: Multifractal spectrum height calculated with Eq. (3).

$$MS_{height} = Dq_{max} - Dq_{min} \qquad (3)$$

F7: Singularity exponent corresponding to maximum multifractal spectrum (hq value corresponding to max Dq value).
F8: Maximum singularity exponent value (hq_{max}).
F9: Minimum singularity exponent value (hq_{min}).
F10: Mean value of singularity exponent values.
F11: Maximum value of multifractal spectrum (Dq_{max}).
F12: Mean value of multifractal spectrum values (Mean Dq).
F13: Multifractal spectrum with left truncation as in Eq. (4) (difference between maximum spectrum value and spectrum value corresponding min singularity exponent).

$$MS_{left} = Dq_{max} - Dq(hq_{min}) \qquad (4)$$

F14: Multifractal spectrum with right truncation as in Eq. (5) (difference between maximum spectrum and spectrum corresponding max singularity exponent).

$$MS_{right} = Dq_{max} - Dq(hq_{max}) \qquad (5)$$

F15: Vertical distance in multifractal spectrum calculated as seen in Eq. (6).

$$MS_{vertical\_dis \tan ce} = Dq(hq_{min}) - Dq(hq_{max}) \qquad (6)$$

F16: Skewness of spectrum.
F17: Kurtosis of spectrum.
F18: Asymmetric index (AI) calculated using Eq. (7) [39]. where σ_0: singularity exponent value corresponding to the maximum of multifractal spectrum.

$$AI = \frac{\Delta\sigma_L - \Delta\sigma_R}{\Delta\sigma_L + \Delta\sigma_R}$$
$$\Delta\sigma_L = \sigma_0 - hq_{min,}$$
$$\Delta\sigma_R = hq_{max} - \sigma_0$$

(7)

F19: Horizontal distance between singularity exponent value corresponding to the maximum of multifractal spectrum and minimum singularity exponent ($\Delta\sigma_L$ in Eq. (7)) [26].

F20: Horizontal distance between singularity exponent value corresponding to the maximum of multifractal spectrum and maximum singularity exponent ($\sigma_0 - hq_{max}$) [26].

F21: Variance of Multifractal Spectrum

F22: Multifractal spectrum corresponding to maximum singularity exponent $Dq(hq_{max})$.

F23: Multifractal spectrum corresponding to minimum singularity exponent $Dq(hq_{min})$.

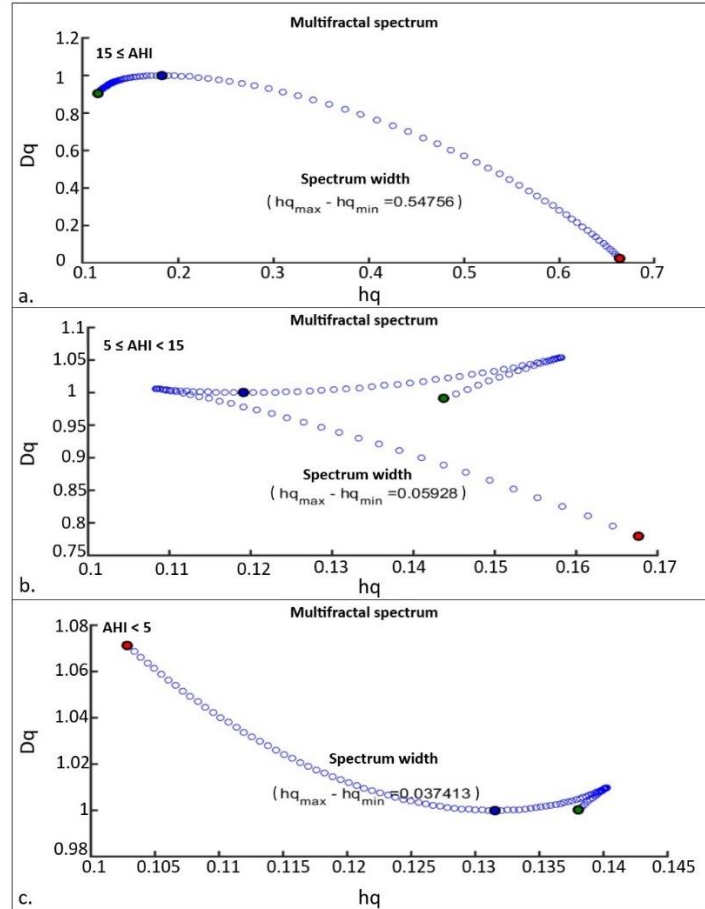Representations of some extracted features from multifractal spectrums are shown in Figure 5.

Figure 4. Multifractal Spectrums, a. Spectrum for 15≤ AHI, b. Spectrum for 5≤ AHI <15, c. Spectrum for AHI <5
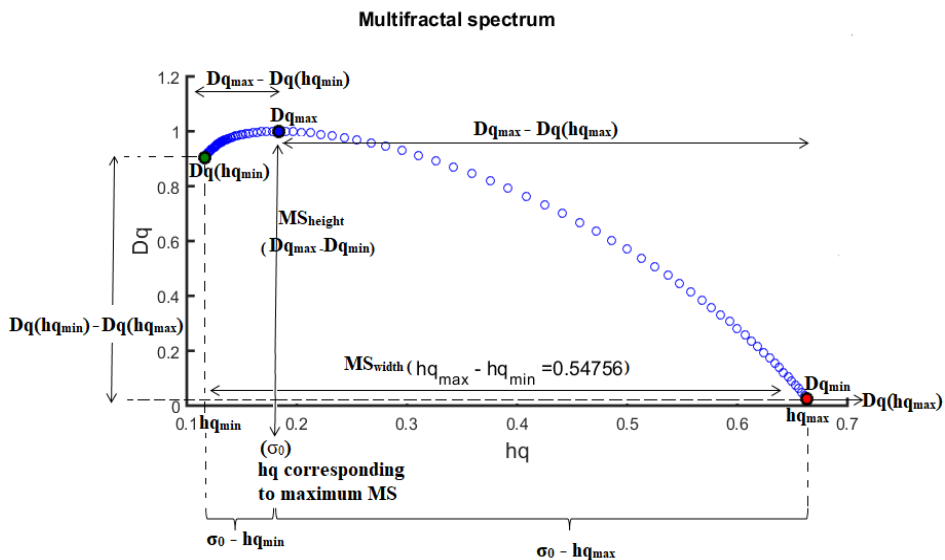

Figure 5. Extracted features from multifractal spectrum

2.5 Feature selection

In general, the performance of the classifier depends on the effectiveness of used features [18]. So, using the features that will separate the different classes at the maximum level will increase the performance of the classifier. Feature selection can be performed either by evaluating each feature independently or by considering the selection of subsets of features with different combinations [40]. In this study, best feature sets were determined by employing different feature selection methods to extracted features of training group.

Preferred methods:

➢ *Information Gain Attribute Evaluation (IG) [41]*: Information gain (relative entropy, or Kullback-Leibler divergence) in probability and information theory is a measure of the difference between two probability distributions. The method evaluates the worth of a feature by measuring the information gain with respect to the class. With the processing with this method, features with highest information gains were selected as most effective.

➢ *Correlation Attribute Evaluation (CAE) [41]*: The method assesses the worth of each feature by measuring the correlation (Pearson's) between it and the class. The purpose of the method to find the subset contain features that are highly correlated with the class and uncorrelated with each other. Features in this subset are called as most effective. The rest of features are ignored, because they will have low correlation with the class.

➢ *OneR Attribute Evaluation (OneR) [42]*: The method calculates the worth of a features using the OneR classification algorithm. The OneR classification algorithm ranks effectiveness of each individual feature by observing error rate and choose the top few to use as most effective.

➢ *Cfs Subset Evaluation (CFS) [40]*: The method measures the worth of a feature subset by considering the individual predictive ability of each feature along with the degree of redundancy between them. A feature subset which is highly correlated with class is accepted as most effective subset.

➢ *Wrapper Subset Evaluation (WSE) [43]*: The method searches an optimal feature subset by using a learning algorithm. Various feature subsets consisting of different combination of features were generated. Each subset is used with determined learning algorithm and the feature subset which ensures the minimum error and highest accuracy is chosen as the final effective set.

The first three of these methods evaluate features independently and determine a feature subset by selecting the most effective features individually. Other two methods evaluate features together by creating subsets with different combination of them and decide best feature subset. These two methods usually provide the best performing feature set compared to other three methods. However, they are very computationally intensive since for each subset needs to be evaluated.

2.6 Classification by Random Forest (RF) classifier algorithm

The RF algorithm suggested by Brierman [44] is an ensemble of decision tree classifiers [45]. A vote of the forest for the final decision and the class of the input is generated by each tree classifier. Then, the RF chooses the classification having the most votes provided by all the trees in the forest

[21]. Detailed explanation of algorithm is given literature [21, 45, 46].

When RF is compared with other classifier algorithms, it is seen that RF has more advantages such as high accuracy, robustness to noise and outliers, easy to cope with over fitting [21]. In addition, this algorithm needs very few parameters to be determined such as number of features (m) to be used for each node and the number of trees (N) to be created [45]. This indicates that RF also has the advantage of implementation simplicity. Therefore, RF classifier algorithm was chosen by this study to classify subjects into three AHI subgroups namely AHI<5, 5≤AHI<15 and 15≤AHI. Since AHI subgroups were determined by RF, subjects were also classified as OSAHS (AHI<5) and nonOSAHS (15≤AHI).

2.7 Metrics of performance analysis

Performance evaluation of the study was carried out through accuracy (AC) as in Eq. (8), the sensitivity (SN) as in Eq. (9), the specificity (SP) as in Eq. (10), the precision or positive predictive value (P or PPV) as in Eq. (11), the F-score (FS) as in Eq. (12) and Kappa statistic measure as in Eq. (13) [21].

$$AC = \frac{TP + TN}{TP + TN + FP + FN} \tag{8}$$

$$SN = \frac{TP}{TP + FN} \tag{9}$$

$$SP = \frac{TN}{TN + FP} \tag{10}$$

$$P(PPV) = \frac{TP}{TP + FP} \tag{11}$$

$$FS = 2 \times \frac{(SN \times P)}{(SN + P)} \tag{12}$$

$$Kappa(K) = \frac{\Pr(\alpha) - \Pr(e)}{1 - \Pr(e)} \tag{13}$$

In Eqns. (8-12), TP express the number of true positives, TN indicates the number of true negatives, FP represents the number of false positives and FN shows the number of false negatives.

In Eq. (13), Pr(α) is the proportion of units where there is agreement and Pr(e) is the proportion of units which would be expected to agree by chance.

3. RESULTS

This study aimed to determine automatically whether 120 subjects suffering from sleep disorders had OSAHS or not and whether they needed PAP therapy or not by identifying their AHI value ranges. The training group consisted of 72 subjects. 38 of them have 15≤ AHI and require PAP therapy, 17 subjects have 5≤ AHI <15 and 17 subjects have AHI values less than 5. The remaining 48 of the 120 subjects constituted the test group.

Each of 5 feature selection methods was applied to the extracted MDFA based features of the training group subjects. The set of effective features revealed by the each of these methods are shown in Table 1. Subsequently, the three-class

classification processes of training and test groups were performed by the RF algorithm with 10-fold cross validation technique using both all extracted features and each effective feature set. In these classifications, the first class is the $15 \leq AHI$. This class represents patients requiring absolutely standard PAP therapy. The second class is the $5 \leq AHI < 15$. This second class specifies patients whose additional information must be examined in order to apply PAP therapy. The third class denotes $AHI < 5$, in other words healthy people who do not require PAP therapy.

Table 1. Effective feature sets

Method	Feature Set	Selected Effective Features	Feature Number
IG	FS1	F2, F3, F4, F8, F9, F10, F20	7
CAE	FS2	F3, F6, F7, F9, F12, F13, F15, F17, F18, F22, F23	11
OneR	FS3	F1, F2, F3, F4, F5, F8, F9, F10, F12	9
CFS	FS4	F3, F4, F9, F12, F23	5
WSE	FS5	F4, F9, F15, F17, F18, F23	6

The classification accuracies and kappa statistical values obtained as a result of the classifications are shown in Table 2. Table 2 also shows the number of trees used in the RF classifier to achieve maximum results for each classification.

Table 2. Classification results according to feature selection algorithms

RF Tree Number	Feature Set	Train		Test	
		AC (%)	K	AC (%)	K
100	All Features	82.35	0.72	72.92	0.60
140	FS1	87.50	0.78	81.00	0.72
90	FS2	84.72	0.74	75.00	0.63
70	FS3	86.11	0.77	77.08	0.66
100	FS4	91.67	0.86	81.25	0.72
80	**FS5**	**93.06**	**0.89**	**93.75**	**0.91**

As presented in Table 2, first classification was realized with all of the 23 features. In this classification, accuracies were obtained as 82.35% and 72.92%, kappa values were acquired as 0.72 and 0.60 for training and test groups, respectively. Then, effective feature sets were created by the feature selection methods and classifications performed by using these sets produced better results with less features.

The first three feature selection methods (*IG-Information Gain Attribute Eval.*, *CAE-Correlation Attribute Eval.* and *OneR-OneR Attribute Eval.*) seen in Table 1 evaluated the features independently and assigned a score to each feature. While the features were selecting with these three methods, firstly, the top 3 features with the highest scores were evaluated by the RF classification algorithm. Then the features were added sequentially according to the effectiveness scores respectively, and the classification process was performed each time by RF. Finally, best feature sets were determined so that it gave maximum classification result. According to this, FS1 set with 7 features, FS2 set with 11 features and FS3 set with 9 features were determined as the best by IG, CAE and OneR methods, respectively. Table 2 shows that among these 3 feature selection methods, the IG method with FS1 set provides the highest accuracy and kappa values for the

classification of test group as 81.00% and 0.72 respectively. CFS (*CFS Subset Eval.*) and WSE (*Wrapper Subset Eval*) selection methods assessed different subsets of the features with Best-First search approach and RF classifier. As a result, they decided the best feature subset that ensured maximum classification accuracy. The FS4 set with 5 features was chosen as the best by CFS method and 81.25% classification accuracy and 0.72 kappa value were achieved in the classification of test group using this set. With the implementation of WSE method, FS5 feature set with 6 features provided the best result and classification performed with this set produced 93.75% classification accuracy and 0.91 kappa values for test group.

Table 2 indicates that evaluating the features together, just like in the CFS and WSE methods, increases the performance than individually evaluation. Moreover, it was seen that 6 features in FS5 set created by WSE method were the most effective features since they provided the highest accuracy and kappa values. These 6 effective features are as follows;

F4: Generalized Hurst exponent

F9: Minimum singularity exponent value (min hq)

F15: Vertical distance between Dq (hq_{min}) and Dq (hq_{max})

F17: Kurtosis of multifractal spectrum

F18: Asymmetric index

F23: Multifractal spectrum corresponding to minimum singularity exponent (Dq (hq_{min}))

The detailed classification results of the training group carried out using FS5 set and RF classifier consisted of 80 tree are given in Table 3.

Table 3. Classification results of training group by using FS5 and RF classifier

Class	SN (%)	SP (%)	P (%)	FS (%)	AC (%)	K
$15 \leq AHI$	94.74	91.18	92.31	93.51		
$5 \leq AHI < 15$	94.12	96.36	88.89	91.43	93.06	0.89
$AHI < 5$	88.24	1	1	93.75		

The detailed classification results obtained for test group by using 6 features in FS5 set and RF algorithm with 80 tree is shown in Table 4. Table 5 presents the confusion matrix of this classification.

Table 4. Classification results of test group by using FS5 and RF classifier

Class	SN (%)	SP (%)	P (%)	FS (%)	AC (%)	K
$15 \leq AHI$	93.75	93.75	88.24	90.91		
$5 \leq AHI < 15$	93.75	100	100	96.77	93.75	0.91
$AHI < 5$	93.75	96.88	93.75	93.75		

Table 5. Confusion Matrix of test group classification

		Predicted		
		$15 \leq AHI$	$5 \leq AHI < 15$	$AHI < 5$
	$15 \leq AHI$	15	0	1
Actual	**$5 \leq AHI < 15$**	1	15	0
	$AHI < 5$	1	0	15

Table 4 demonstrated that 93.75% sensitivities were achieved for all AHI subgroups of test group. 93.75%, 100% and 96.88% specificities were obtained for $15 \leq AHI$, $5 \leq AHI < 15$ and $AHI < 5$ subgroups, respectively. This

classification had also high F-Scores for each subgroup to be higher than 90%.

As seen from confusion matrix in Table 5, it was correctly decided that treatment with PAP therapy is absolutely necessary for 15 subjects in 15≤AHI subgroup. Only one subject in this subgroup was misclassified. So, decision of PAP therapy was given incorrectly for this subject. For 15 subjects in 5≤AHI<15 subgroup, it was concluded that additional information was needed proposed by CMS [6] to decide treatment with PAP therapy. Therefore, this decision was left to sleep specialists to investigate additional information associated with these subjects. For one misclassified subject in this group, treatment with PAP therapy was considered necessary without the need for sleep specialist opinion and wrong decision was given. 15 subjects in AHI<5 subgroup were correctly defined as those who did not require PAP therapy. As in the other groups, one subject was misclassified in this group and therefore the PAP therapy decision was given wrong.

In total, 32 subjects in the test group have OSAHS since their AHI values are greater than or equal 5. 16 subjects are healthy. According to Table 5, it could be said that AHI value of one patient among 32 OSAHS patients was identified as less than 5, that is, this patient was misclassified as healthy. Likewise, one subject of 16 healthy subjects was misclassified as OSAHS patient since AHI subgroup of this subject was determined as 15≤AHI. Hence, accuracy, sensitivity and specificity metrics used for distinguishing patients from healthy individuals were obtained as 95.83%, 96.88% and 93.75%, respectively.

3.1 Comparison with the other classifiers

In this study, to prove the robustness of RF classifier with the most successfully feature set, SVM, ANN and Naive Bayes (NB) which were commonly preferred classifiers in literature were chosen and experiments were performed for three classes (15≤AHI, 5≤AHI<15 and AHI<5). As a result of this experiments, since the different AHI subgroups were determined, results were also assessed for two classes (OSAHS=5≤AHI and non-OSAHS=AHI<5). The classification performances of RF, SVM, ANN and NB were compared by using FS5 feature set for training and test subjects. Table 6 and Table 7 show the classification accuracies and kappa statistical values obtained from three-class and two-class classifications, respectively.

Table 6. Three–class classification results of RF and three different classifiers

| Classifier | Three-class (15≤AHI, 5≤AHI<15, AHI<5) | | | |
| | Train | | Test | |
	AC (%)	K	AC (%)	K
RF (Tree:80)	93.06	0.89	93.75	0.91
SVM C:17, PolyKernel	76.39	0.58	62.50	0.44
ANN lr:0.1, mc:0.09 Iteration:1200	72.00	0.54	70.00	0.56
NB	64.71	0.42	60.00	0.42

lr: learning rate, mc: momentum coefficient

It could be seen in Table 6 and Table 7 that, the highest AC values were obtained with RF classifier as 93.75% and 95.83% for test group subjects, respectively. In addition, the use of RF

provided the generation of the highest K values as 0.91 both three and two classes. ANN classifier produced performance moderately. Other classifiers SVM and NB had the lower performance than RF and ANN in terms of both AC and K values.

Table 7. Two–class classification results of RF and three different classifiers

| Classifier | Two-class (OSAHS, non-OSAHS) | | | |
| | Train | | Test | |
	AC (%)	K	AC (%)	K
RF (Tree:80)	97.22	0.92	95.83	0.91
SVM C:17, PolyKernel	86.11	0.58	77.08	0.46
ANN lr:0.1, mc:0.09 Iteration:1200	81.94	0.66	83.33	0.61
NB	80.88	0.41	70.00	0.33

lr: learning rate, mc: momentum coefficient

4. DISCUSSIONS

OSAHS is a serious sleep disorder that negatively affects people's lives. The definitive diagnosis of OSAS is performed by determining 5≤AHI by PSG with the help of a sleep specialist in the laboratory. People are asked to spend a night in the laboratory for this diagnosis. Then, people with AHI values greater than or equal to 15 are asked to spend another night in the laboratory for PAP treatment. If anyone with AHI values between 5 and 15 has additional symptoms such as hypertension, cardiac arrhythmias, excessive daytime sleepiness, focusing problem, PAP treatment is recommended and this patient spends one more night in the laboratory. These processes are time consuming, laborious, boring, exhausting and person-dependent. Moreover, sleep laboratory and number of beds are limited in some places in the world. Therefore, this study focused on the automatic diagnosis of OSASH and determination the need for PAP therapy.

In literature, nonlinear and fractal structure of sleep, OSAHS and recorded signals during sleep have been examined by many researchers [5, 7, 29, 30, 47]. Kaimakamis et al. [5] studied with 86 patients. They extracted Largest Lyapunov Exponent (LLE), Approximate Entropy (ApEn) and Detrended Fluctuation Analysis (DFA) based two features from two respiratory signals including nasal cannula flow and thoracic belt-T as nonlinear indices. Using DFA, extracted two features were DFA fast value which represented the power law slope on the medium to fast time scales and the DFA slow value, i.e. the slope on the slow to medium time scales. Also, besides these respiratory signals, the SpO2 signal was selected in their study and time features were extracted from this signal. They preferred C4.5 decision tree as a machine learning algorithm. The discrimination between normal subjects and OSAS patients presented an accuracy of 84.9% and a sensitivity of 90.3% using the variables age, sex, two DFA features from nasal airflow and time of SpO2 oxygen value<90%. The classification of patients into severity groups (AHI<5, 5≤AHI<15, 15≤AHI<30 and 30≤AHI) had an accuracy of 74.2% and a sensitivity of 81.1% using the variables ApEn and two DFA features from nasal airflow and time with SpO2 oxygen value <90% [5]. Same researchers Kaimakamis et al. [47] carried out another study with 135 subjects. They extracted same nonlinear features LLE, DFA and ApEn from nasal cannula airflow, thoracic movement

signals and one linear feature derived from SpO2 signal to predict AHI values of patients. They created both linear regression and C4.5 decision tree model for prediction. Linear regression model presented a correlation coefficient of 0.77 in predicting AHI. With a cutoff value of AHI = 8, the sensitivity and specificity were 93% and 71.4% in discrimination between patients and normal subjects. The decision tree for the discrimination between patients and normal had sensitivity and specificity of 91% and 60%, respectively [47]. Vaquerizo-Villar et al. [7] performed DFA of the SpO2 to assist in paediatric sleep apnea-hypopnea syndrome diagnosis. 981 blood SpO2 signals of children was used in their study to extract DFA-derived features in order to quantify the scaling behaviour and the fluctuations of the signal. They also computed the 3% oxygen desaturation index (ODI3) for each subject. Fast correlation-based filter (FCBF) select ODI3 and the slope in the first scaling region of the DFA as most effective features. Selected features were used to feed MLP to estimate the AHI. In their study, the estimated AHI showed high diagnostic ability, reaching 82.7%, 81.9%, and 91.1% accuracies using three common AHI cut-off 1, 5, and 10 events per hour respectively [7]. Da Silva et al. [29] aimed at investigating a heart rate variability (HRV) of 47 subjects for early diagnosis of OSAHS. HRV was studied by linear measures of fast Fourier transform, nonlinear Poincaré analysis, and DFA. For their study, the ROC analysis revealed that DFA based feature predicted moderate and severe OSA with a sensitivity/specificity/area under the curve of 86%/64%/0.8 and 60%/89%/0.76, respectively [29]. Deng et al. [30] studied the diagnostic potential of HRV in pediatric sleep apnea using power spectral analysis (PSA), numerical titration (NT), SamEn, and DFA. They found that NT technique was more effective than other techniques to detect OSAHS. With the using this technique, researchers yielded a

specificity of 72.2% and sensitivity of 81.3% for OSAHS detection. All off these studies revealed that nonlinear features of physiological signals are significantly correlated with OSAHS.

DFA technique, one of the non-linear techniques, was preferred by many previous studies and stated as effective for OSAHS [5, 7, 29, 30, 47]. However, until now, MDFA which is the advanced version of DFA has not been used in any study that deals with OSAHS. Whereas, it has been known that many physiological signals have multifractal structure and cannot be represented only a fractal provided by methods such as DFA. Therefore, some researches preferred MDFA technique and analyzed different pathological conditions using various physiological signals such as EEG, ECG and heart sounds. As a result, in this study, it was considered that single channel airflow signals indicated multifractal structure and had variations, spikes and irregular fluctuations arising from apnea and hypopnea events of OSAHS patients. Therefore, it was believed that analysis of these signals by MDFA provided additional information to clinicians related to OSAHS. In this context, single channel nasal cannula airflow signals of subjects were analyzed with MDFA technique and novel 23 features were extracted to identify the subjects' AHI subgroups. 6 of these features have been selected by the WSE method as the most effective features on AHI subgroups. With the use of RF classifier algorithm and these effective features, subjects were assigned to one of the AHI subgroups with either AHI<5 or 5≤AHI<15 or 15≤AHI. Thus, it was determined whether the subjects were OSAHS or not and whether they needed PAP treatment or not.

Table 8 compares the performance of this study and other studies that deals with similar problems by adopting DFA and additional techniques together with one or more physiological signals.

Table 8. Literature studies

Researchers	Used Signals	Method	Performance
Kaimakamis et al. [5]	Nasal airflow, Thoracic flow, SpO2	LLE, DFA, ApEn, C4.5	Accuracy for OSASH diagnosis: 84.9% Accuracy for OSAHS severity: 74.2%
Kaimakamis et al. [47]	Nasal cannula airflow, Thoracic movement, SpO2	LLE, DFA, ApEn LR, DT	With a cutoff value of AHI = 8, the sensitivity and specificity were obtained as 93% and 71.4% in discrimination between patients and normal subjects by using linear regression. The decision tree for the discrimination between patients and normal had sensitivity and specificity of 91% and 60%, respectively.
Vaquerizo-Villar et al. [7]	SpO2	ODI3, DFA MLP	82.7%, 81.9%, and 91.1% accuracies were obtained for paediatric AHI cut-offs of 1, 5, and 10 events per hour, respectively.
Da Silva et al. [29]	Heart rate	DFA	Moderate OSAHS with 86.11% sensitivity and severe OSAHS with 63.64 % sensitivity were predicted.
Deng et al. [30]	Heart rate	DFA, PSA, NT, SamEn	In paediatric OSAS diagnosis, 72.2% specificity and 81.3% sensitivity were obtained.
This study	Nasal cannula airflow	MDFA RF	93.75 % accuracy and 0.91 kappa value were obtained in the determination of different AHI subgroups. 93.75% sensitivities were obtained for 15≤ AHI, 5≤ AHI <15 and AHI<5 subgroups. 95.83% accuracy, 0.91 kappa value, 96.88% sensitivity and 93.75% specificity were obtained in the discrimination of OSAHS and nonOSAHS. 0.90

RF: Random Forest, LLE: Largest Lyapunov Exponent, ApEn: Approximate Entropy, LR: Linear Regression, DT: Decision Tree, ODI3: Oxygen Desaturation Index, PSA: Power Spectral Analysis, NT: Numerical Titration, SamEn: Sample entropy, DFA: Detrended Fluctuation Analysis, MDFA: Multifractal Detrended Fluctuation Analysis. MLP: Multi-Layer Perceptron

When the Table 8 was examined, it could be seen that the overall performance of this study was better than that of similar studies in the literature in terms of discrimination between OSAHS patients and normal subjects with 95.83% accuracy, 96.88% sensitivity and 93.75% specificity. This

study also provided high performance in differentiating patients who need or did not need PAP therapy. The sensitivity values for each of the subgroups namely 15≤ AHI, 5≤AHI<15 and AHI<5 was obtained as 93.75%. In addition, unlike the previous studies, this study used only single channel nasal

cannula airflow signal and only MDFA technique. Nevertheless, this study showed higher performance than previous studies used more than one signals and techniques. This pointed that the proposed technique (MDFA) was capable of distinguishing between healthy subjects and OSAHS patients more accurately. This is because, since several new features were extracted with this technique, they could capture small fluctuations and variations occurring in nasal cannula airflow signals more accurately. In the clinical environment, nasal cannula airflow signals and changes arising in them play a key role for diagnosis and treatment of OSAHS by sleep specialists. In this study, as the changes in nasal airflow signals were evaluated easily by MDFA technique, higher performances were obtained without the need for any other nonlinear technique and any other physiological signal.

5. CONCLUSIONs

This study investigated effectiveness of multifractal analysis of nasal cannula airflow signals on OSAHS. At the end of the study, it was seen that 6 of the 23 features extracted by MDFA technique had ability to identify different AHI subgroups of OSAHS and thereby determine OSAHS patients and those who need PAP therapy. This revealed that multifractal analysis was very effective in making decisions about OSAHS just like other pathological conditions.

By using this study's proposed features, only single-channel airflow signals without the need of other physiological signals and RF classifier algorithm, a low cost PSG device can be developed for patients to use in their own home. In this way, it can be automatically determined whether people have OSAHS or not and whether OSAHS patients need PAP therapy or not. Thus, the need to stay in the laboratory more than one night can be eliminated and time and cost can be saved.

REFERENCES

[1] El Solh, A.A., Aldik, Z., Alnabhan, M., Grant, B. (2007). Predicting effective continuous positive airway pressure in sleep apnea using an artificial neural network. Sleep Medicine, 8(5): 471-477. http://dx.doi.org/10.1016/j.sleep.2006.09.005

[2] Krieger, J., Kurtz, D., Petiau, C., Trautmann, D. (1996). Long-term compliance with CPAP therapy in obstructive sleep apnea patients and in snorers. Sleep, 19(9): 136-143. http://dx.doi.org/10.1093/sleep/19.suppl_9.S136

[3] Basoglu, O.K., Tasbakan, M.S. (2012). Determination of new prediction formula for nasal continuous positive airway pressure in Turkish patients with obstructive sleep apnea syndrome. Sleep Breath, 16(4): 1121-1127. http://dx.doi.org/10.1007/s11325-011-0612-z

[4] Donovan, L.M., Boeder, S., Malhotra, A., Patel, S.R. (2015). New developments in the use of positive airway pressure for obstructive sleep apnea. Journal of Thoracic Disease, 7(8): 1323-1342. https://dx.doi.org/10.3978/j.issn.2072-1439.2015.07.30

[5] Kaimakamis, E., Bratsas, C., Sichletidis, L., Karvounis, C., Maglaveras, N. (2009). Screening of patients with obstructive sleep apnea syndrome using C4.5 algorithm based on non linear analysis of respiratory signals during sleep. Proc. 2009 Annual International Conference of the IEEE Engineering in Medicine and Biology Society, Minneapolis, MN, USA, pp. 3465-3469. http://dx.doi.org/10.1109/IEMBS.2009.5334605

[6] CMS Manual system. (2005). www.cms.hhs.gov/Transmittals/Downloads/R35NCD.pdf, accessed on 25 December 2019.

[7] Vaquerizo-Villar, F., Alvarez, D., Kheirandish-Goza, L., Gutiérrez-Tobal, G.C., Barroso-García, V., Crespo, A., Campo, F.D., Gozal, D., Hornero, R. (2018). Detrended fluctuation analysis of the oximetry signal to assist in paediatric sleep apnoea-hypopnoea syndrome diagnosis. Physiological Measurement, 39(11): 114006. http://dx.doi.org/10.1088/1361-6579/aae66a

[8] American Academy of Seep Medicine, The AASM Manual for the Scoring of Sleep and Associated Events, Version v2.0. (2012). https://aasm.org/clinical-resources/scoring-manual/, accessed on 18 January 2019.

[9] Collop, N.A. (2002). Scoring variability between polysomnography technologists in different sleep laboratories. Sleep Medicine, 3(1): 43-47. http://dx.doi.org/10.1016/S1389-9457(01)00115-0

[10] Lee, H., Park, J., Kim, H., Lee, K.J. (2016). New rule-based algorithm for real-time detecting sleep apnea and hypopnea events using a nasal pressure signal. Journal of Medical Systems, 40(12): 282. http://dx.doi.org/10.1007/s10916-016-0637-8

[11] Varady, P., Micsik, T., Benedek, S., Benyo, Z. (2002). A novel method for the detection of apnea and hypopnea events in respiration signals. IEEE Transactions on Biomedical Engineering, 49(9): 936-942. http://dx.doi.org/10.1109/TBME.2002.802009

[12] Tian, J.Y., Liu, J.Q. (2005). Apnea detection based on time delay neural network. IEEE Engineering in Medicine and Biology 27th Annual Conference, Shanghai, pp. 2571-2574. http://dx.doi.org/10.1109/IEMBS.2005.1616994

[13] Nakano, H., Tanigawao, T., Furukawa, T., Nishima, S. (2007). Automatic detection of sleep-disordered breathing from a single-channel airflow record. European Respiratory Journal, 29(4): 728-736. http://dx.doi.org/10.1183/09031936.00091206

[14] Salisbury, J.I., Sun, Y. (2007). Rapid screening test for sleep apnea using a nonlinear and nonstationary signal processing technique. Medical Engineering & Physics, 29(3): 336-343. http://dx.doi.org/10.1016/j.medengphy.2006.05.013

[15] Rathnayake, S.I., Wood, I.A., Abeyratne, U.R., Hukins, C. (2010). Nonlinear features for single-channel diagnosis of sleep-disordered breathing diseases. IEEE Transactions on Biomedical Engineering, 57(8): 1973-1981. http://dx.doi.org/10.1109/TBME.2010.2044175

[16] Almazaydeh, L., Elleithy, K., Faezipour, M., Abushakra, A. (2013). Apnea detection based on respiratory signal classification. Procedia Computer Science, 21: 310-316. http://dx.doi.org/10.1016/j.procs.2013.09.041

[17] Jayasri, T., Hemalatha, M. (2013). Categorization of respiratory signal using ANN and SVM based on feature

extraction algorithm. Indian Journal of Science and Technology, 6(9): 5195-5200. https://dx.doi.org/10.17485/ijst/2013/v6i9/37144

[18] Koley, B.L., Dey, D. (2013). Automatic detection of sleep apnea and hypopnea events from single channel measurement of respiration signal employing ensemble binary SVM classifiers. Measurement, 46(7): 2082-2092. http://dx.doi.org/10.1016/j.measurement.2013.03.016

[19] Selvaraj, N., Narasimhan, R. (2013). Detection of sleep apnea on a per-second basis using respiratory signals. IEEE Engineering in Medicine and Biology, pp. 2124-2127. http://dx.doi.org/10.1109/EMBC.2013.6609953

[20] Moret-Bonillo, V., Alvarez-Estevez, D., Fernandez-Leal, A., Hernandez-Pereira, E. (2014). Intelligent approach for analysis of respiratory signals and oxygen saturation in the sleep apnea/hypopnea syndrome. Open Medical Informatics Journal, 8: 1-19. http://dx.doi.org/10.2174/1874431101408010001

[21] Avci, C., Akbas, A. (2015). Sleep apnea classification based on respiration signals by using ensemble methods. Bio-Medical Materials and Engineering, 26(1): 1703-1710. http://dx.doi.org/10.3233/BME-151470

[22] Ciolek, M., Niedzwiecki, M., Sieklicki, S., Drozdowski, J., Siebert, J. (2015). Automated detection of sleep apnea and hypopnea events based on robust airflow envelope tracking in the presence of breathing artifacts. IEEE Journal of Biomedical and Health Informatics, 19(2): 418-429. http://dx.doi.org/10.1109/JBHI.2014.2325997

[23] Huang, W., Guo, B., Shen, Y., Tang, X. (2017). A novel method to precisely detect apnea and hypopnea events by airflow and oximetry signals. Computers in Biology and Medicine, 88: 32-40. http://dx.doi.org/10.1016/j.compbiomed.2017.06.015

[24] Choi, S.H., Yoon, H., Kim, H.S., Kim, H.B., Kwon, H.B., Oh, S.M., Lee, Y.J., Park, K.S. (2018). Real-time apnea-hypopnea event detection during sleep by convolutional neural networks. Computers in Biology and Medicine, 100: 123-131. http://dx.doi.org/10.1016/j.compbiomed.2018.06.028

[25] Koley, B., Dey, D. (2012). An ensemble system for automatic sleep stage classification using single channel EEG signal. Computers in Biology and Medicine, 42(12): 1186-1195. http://dx.doi.org/10.1016/j.compbiomed.2012.09.012

[26] Bose, R., Pratiher, S., Chatterjee, S. (2019). Detection of epileptic seizure employing a novel set of features extracted from multifractal spectrum of electroencephalogram signals. IET Signal Processing, 13(2): 157-164. http://dx.doi.org/10.1049/iet-spr.2018.5258

[27] Azmy, M.M., Mohamady, R. (2017). Heart sounds recognition using multifractal detrended fluctuation analysis and support vector machine. Proc. IEEE Jordan Conference on Applied Electrical Engineering and Computing Technologies (AEECT), Aqaba, pp. 1-4. http://dx.doi.org/10.1109/AEECT.2017.8257742

[28] Dutta, S., Ghosh, D., Chatterjee, S. (2013). Multifractal detrended fluctuation analysis of human gait diseases. Frontiers in Physiology, 4: 274. http://dx.doi.org/10.3389/fphys.2013.00274

[29] Da Silva, E.L., Pereira, R., Reis, L.N., Pereira, V.L., Jr., Campos, L.A., Wessel, N., Baltatu, O.C. (2015). Heart rate detrended fluctuation indexes as estimate of obstructive sleep apnea severity. Medicine (Baltimore),

94(4): 516. http://dx.doi.org/10.1097/MD.0000000000000516

[30] Deng, Z., Poon, C., Arzeno, N.M., Katz, E.S. (2006). Heart rate variability in pediatric obstructive sleep apnea. Proceedings of the 28th IEEE EMBS Annual International Conference, New York City, USA, pp. 3565-3568. http://dx.doi.org/10.1109/IEMBS.2006.260139

[31] Diaz, J.A., Arancibia, J.M., Bassi, A., Vivaldi, E.A. (2014). Envelope analysis of the airflow signal to improve polysomnographic assessment of sleep disordered breathing. Sleep, 37(1): 199-208. http://dx.doi.org/10.5665/sleep.3338

[32] Peng, C.K., Havlin, S., Stanley, H.E., Goldberger, A. (1995). Quantification of scaling exponents and crossover phenomena in nonstationary heartbeat time series. Chaos, 5(1): 82-87. http://dx.doi.org/10.1063/1.166141

[33] Kantelhardt, J.W., Zschiegner, S.A., Koscielny-Bunde, E., Havlin, S., Bunde, A., Stanley, H.E. (2002). Multifractal detrended fluctuation analysis of nonstationary time series. Physica A: Statistical Mechanics and its Applications, 316: 87-114. https://dx.doi.org/10.1016/S0378-4371(02)01383-3

[34] Chen, Z., Ivanov, P., Hu, K., Stanley, H.E. (2002). Effect of nonstationarities on detrended fluctuation analysis. Physical Review E, 65: 041107. http://dx.doi.org/10.1103/PhysRevE.65.041107

[35] Ihlen, E.A. (2012). Introduction to multifractal detrended fluctuation analysis in matlab. Frontiers in Physiology, 3: 141. http://dx.doi.org/10.3389/fphys.2012.00141

[36] Pratiher, S., Chatterjee, S., Bose, R. (2017). Automated diagnosis of epilepsy employing multifractal detrended fluctuation analysis based features. https://arxiv.org/ftp/arxiv/papers/1704/1704.01297.pdf.

[37] Márton, L.F., Brassai, S.T., Bakó, L., Losonczi, L. (2014). Detrended fluctuation analysis of EEG signals. Procedia Technology, 12: 125-132. http://dx.doi.org/10.1016/j.protcy.2013.12.465

[38] Lashermes, B., Abry, P., Chainais, P. (2011). New insights into the estimation of scaling exponents. International Journal of Wavelets Multiresolution and Information Processing, 2(4): 497-523. http://dx.doi.org/10.1142/S0219691304000597

[39] Li, Q.S., Xie, W.X., Huang, J.X. (2015). Multifractal spectrum features based classification method for aircraft. Proc. IET International Radar Conference, Hangzhou, 1-6. http://dx.doi.org/10.1049/cp.2015.0961

[40] Xie, B.L., Minn, H. (2012). Real-time sleep apnea detection by classifier combination. IEEE Transactions on Information Technology in Biomedicine, 16(3): 469-477. http://dx.doi.org/10.1109/TITB.2012.2188299

[41] Yildirim, P. (2015). Filter based feature selection methods for prediction of risks in hepatitis disease. International Journal of Machine Learning and Computing, 5(4): 258-263. http://dx.doi.org/10.7763/IJMLC.2015.V5.517

[42] Gogus, F.Z., Tezel, G. (2019). Apneic events detection using different features of airflow signals. Mehran University Research Journal of Engineering and Technology, 38(1): 1-16. https://dx.doi.org/10.22581/muet1982.1901.01

[43] Yucelbas, S., Yucelbas, C., Tezel, G., Ozsen, S., Yosunkaya, S. (2018). Automatic sleep staging based on

SVD, VMD, HHT and morphological features of single-lead ECG signal. Expert Systems with Applications, 102: 193-206. http://dx.doi.org/10.1016/j.eswa.2018.02.034

[44] Breiman, L. (2001). Random forests. Machine Learning, 45: 5-32. https://doi.org/10.1023/A:1010933404324

[45] Akkoc, B., Arslan, A., Kok, H. (2017). Automatic gender determination from 3D digital maxillary tooth plaster models based on the random forest algorithm and discrete cosine transform. Computer Methods and Programs in Biomedicine, 143: 59-65. http://dx.doi.org/10.1016/j.cmpb.2017.03.001

[46] Akkoc, B., Arslan, A., Kok, H. (2016). Gray level co-occurrence and random forest algorithm-based gender determination with maxillary tooth plaster images. Computers in Biology and Medicine, 73: 102-107. http://dx.doi.org/10.1016/j.compbiomed.2016.04.003

[47] Kaimakamis, E., Tsara, V., Bratsas, C., Sichletidis, L., Karvounis, C., Maglaveras, N. (2016). Evaluation of a decision support system for obstructive sleep apnea with nonlinear analysis of respiratory signals. Plos One, 11(3). http://dx.doi.org/10.1371/journal.pone.0150163